





Cite this: *RSC Adv.*, 2022, 12, 34704

Synthesis of chiral-at-metal rhodium complexes from achiral tripodal tetradentate ligands: resolution and application to enantioselective Diels–Alder and 1,3-dipolar cycloadditions†

Alvaro G. Tejero, María Carmona, Ricardo Rodríguez, * Fernando Viguri,*
Fernando J. Lahoz,  Pilar García-Orduña  and Daniel Carmona *

An improved synthesis of the racemic rhodium compound $[\text{RhCl}_2(\kappa^4\text{C},\text{N},\text{N}',\text{P}-\text{L1})]$ (**1**) containing an achiral tripodal tetradentate ligand is reported. Their derived solvate complexes $[\text{Rh}(\kappa^4\text{C},\text{N},\text{N}',\text{P}-\text{L1})(\text{Solv})_2][\text{SbF}_6]_2$ ($\text{Solv} = \text{NCMe}$, **2**; H_2O , **3**) are resolved into their two enantiomers. Complexes **2** and **3** catalyze the Diels–Alder (DA) reaction between methacrolein and cyclopentadiene and the 1,3-dipolar cycloaddition reaction between methacrolein and the nitron *N*-benzylidenphenylamine-*N*-oxide. When enantiopure ($A_{\text{Rh}}, R_{\text{N}}$)-**2** was employed as the catalyst, enantiomeric ratios $>99/1$, in the *R* at C2 adduct, and up to 94/6, in the 3,5-*endo* isomer, were achieved in the DA reaction and in the 1,3-dipolar cycloaddition reaction, respectively. A plausible catalytic cycle that accounts for the origin of the observed enantioselectivity is proposed.

Received 3rd November 2022
Accepted 23rd November 2022

DOI: 10.1039/d2ra06982b

rsc.li/rsc-advances

Introduction

Typically, a homogeneous chiral metal catalyst consists of a metal surrounded by a chiral ligand and accompanied by a range of achiral ligands. The source of chirality is the chiral ligand which configures a “chiral pocket” in the vicinity of the metal where the reaction between the catalytic substrates takes place.¹

As early as 1979, Brunner argued: “*It therefore seemed promising to move the inducing chirality to the metal atom where the catalysis is occurring*”.² However, in 2000, 21 years later, Muñiz and Bolm recognized that asymmetric catalysis with enantiomeric chiral-at-metal complexes was still unknown and that the only approach to this type of catalysts was diastereomeric complexes in which the configuration of the metal centre is pre-determined by the coordination of a chiral ligand.³

It is interesting to point out that enantiomerically pure coordination compounds have been known since 1911 when Werner reported the resolution of the complex $[\text{Co}(\text{en})_2(\text{X})]^{2+}$ ($\text{en} = \text{ethylenediamine}$, $\text{X} = \text{Cl}$ or Br) into the individual mirror-imaged Δ - and Λ -enantiomers.⁴ However, it should be

noted that the design and synthesis of efficient enantiopure catalysts in which the only stereogenic centre is the metal is not exempt from difficulties. On the one hand, given that different structural isomers are usually possible, the most suitable isomer must be selectively prepared or separated from the obtained mixture. In addition, this isomer will be obtained as a racemate that must be resolved following protocols that generally require a great deal of time with no guarantee of success.⁵ On the other, for these catalysts to achieve high efficiency, it is very convenient that they meet two requirements that seem contradictory *a priori*: configurational stability and labile coordination positions. Most likely for these reasons, the systematic development of chiral-only-at-metal catalysts has occurred only very recently. Indeed, although in 2003, Fontecave *et al.* demonstrated for the first time that chiral-only-at-metal bis-diimine $\text{Ru}(\text{II})$ complexes catalyze the oxidation of sulfides to sulfoxides by hydrogen peroxide with up to 59/41 er,⁶ only since 2013 the synthesis, resolution and catalytic applications of stereogenic-only-at-metal chiral catalysts has been systematically developed. From this date, Meggers group and others have been developing a family of bis-cyclometalated octahedral rhodium(III), iridium(III), ruthenium(II) and iron(II) complexes that efficiently catalyze a variety of organic transformations following Lewis acid,⁷ ligand sphere mediated^{7b-e,8} and photoredox^{7b-e,9} catalytic protocols.

Also in this line, Gladysz's group reported that octahedral enantiopure salts of the tris-chelate ethylenediamine complexes $[\text{M}(\text{en})_3][\text{Barf}]_n$ ($\text{M} = \text{Co}$, Cr , Rh , Ir , $n = 3$; $\text{M} = \text{Pt}$, $n = 4$; $\text{Barf} = \text{B}(3,5\text{-C}_6\text{H}_3(\text{CF}_3)_2)_4$) catalyze the addition of malonates to

Departamento de Catálisis y Procesos Catalíticos, Instituto de Síntesis Química y Catálisis Homogénea (ISQCH), CSIC – Universidad de Zaragoza, Pedro Cerbuna 12, 50009 Zaragoza, Spain. E-mail: dcarmona@unizar.es; riromar@unizar.es; fviguri@unizar.es

† Electronic supplementary information (ESI) available: NMR spectra of complexes **2**–**4**, HPLC chromatograms, and spectroscopic and structural characterization of complex **2**. CCDC 2206804. For ESI and crystallographic data in CIF or other electronic format see DOI: <https://doi.org/10.1039/d2ra06982b>



cyclopentenone or *trans*- β -nitrostyrene and that of the methyl 2-oxocyclopentanecarboxylate to di-*tert*-butylazodicarboxylate following a second coordination sphere mechanism involving substrate activation by hydrogen bonding to the coordinate NH_2 units. Modest enantioselectivities were achieved in all cases.¹⁰ Also, pseudo-octahedral geometry presents an enantiopure chiral-at-ruthenium complex containing a cyclometalated chelating NHC ligand that efficiently catalyzes the asymmetric cross metathesis, asymmetric ring closing metathesis and asymmetric ring opening cross metathesis of olefins.¹¹

On the other hand, tetrahedral complexes with stereogenic metal centres are rarely used as chiral catalysts mainly because they are too labile to ensure the absolute configuration of the metal centre. However, Shionoya *et al.* have reported the preparation and resolution of the tetrahedral chiral zinc complex **1** with high configurational stability using the achiral tridentate ligand **H₂L** depicted in Scheme 1. When enantiopure **S-I** was applied to the asymmetric oxa-Diels–Alder reaction of Danishefsky's diene with 1-naphthaldehyde the Diels–Alder *R*-adduct was obtained in 98% yield with 93.5/6.5 er.¹²

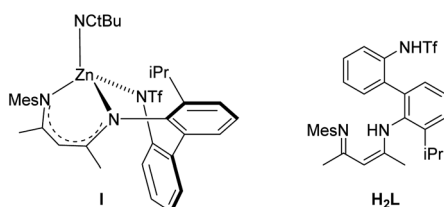
We have recently reported the application of achiral tripodal tetradentate ligands to the synthesis of octahedral chiral-at-metal rhodium, iridium and ruthenium complexes.¹³ In particular, enantiopure rhodium complexes efficiently catalyze the enantioselectively Diels–Alder reaction between methacrolein and cyclopentadiene with enantiomeric ratios of up to >99/1 (ref. 13c) and, on the basis of experimental NMR studies and DFT calculations, a detailed mechanistic pathway for the Friedel–Crafts reaction of *trans*- β -nitrostyrene and *N*-methyl-2-methylindole reaction is proposed, including an explanation of the origin of the obtained enantioselectivity.^{13a}

Herein, we report on the synthesis and stereochemical resolution of the rhodium complex **2** containing the tripodal tetradentate **L1** (Scheme 2) and its application to enantioselective Diels–Alder and 1,3-dipolar cycloadditions.

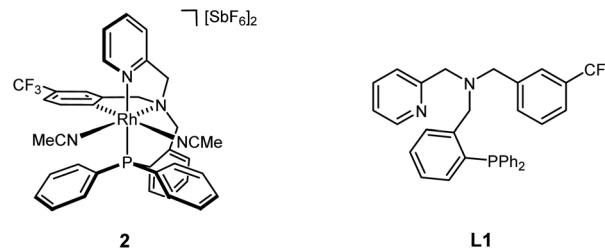
Results and discussion

Synthesis of neutral dichloride complex $[\text{RhCl}_2(\kappa^4\text{C},\text{N},\text{N}',\text{P}-\text{L1})]$ (**1**)

The achiral tripodal tetradentate ligand **L1** has been prepared as reported elsewhere.^{13e} The synthesis of the dichlorido complex $[\text{RhCl}_2(\kappa^4\text{C},\text{N},\text{N}',\text{P}-\text{L1})]$ (**1**) has been previously accomplished following the three steps protocol **A** depicted in Scheme 3.^{13e} Reaction of RhCl_3 with the ligand **L1** in refluxing ethanol affords a mixture of *fac*-OC-6-43 (ref. 14) and *mer*-OC-6-41



Scheme 1 Chiral at zinc tetrahedral complex **1** and the achiral ligand **H₂L**.



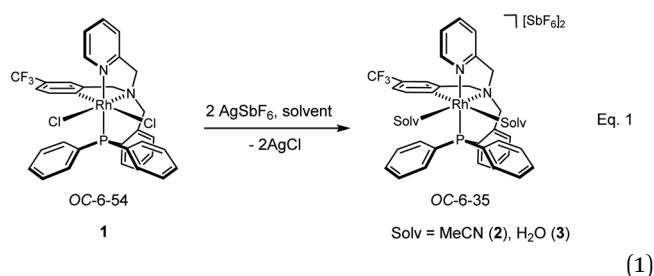
Scheme 2 Chiral rhodium complex **2** bearing the achiral ligand **L1**.

trichlorido isomers that can be completely isomerized to the *fac* diastereomer by refluxing the mixture overnight in the same solvent. The cyclometalated isomer OC-6-54 of the dichlorido complex **1** could be obtained by refluxing in methanol pure trichlorido *fac*-OC-6-43 in the presence of NaOAc.

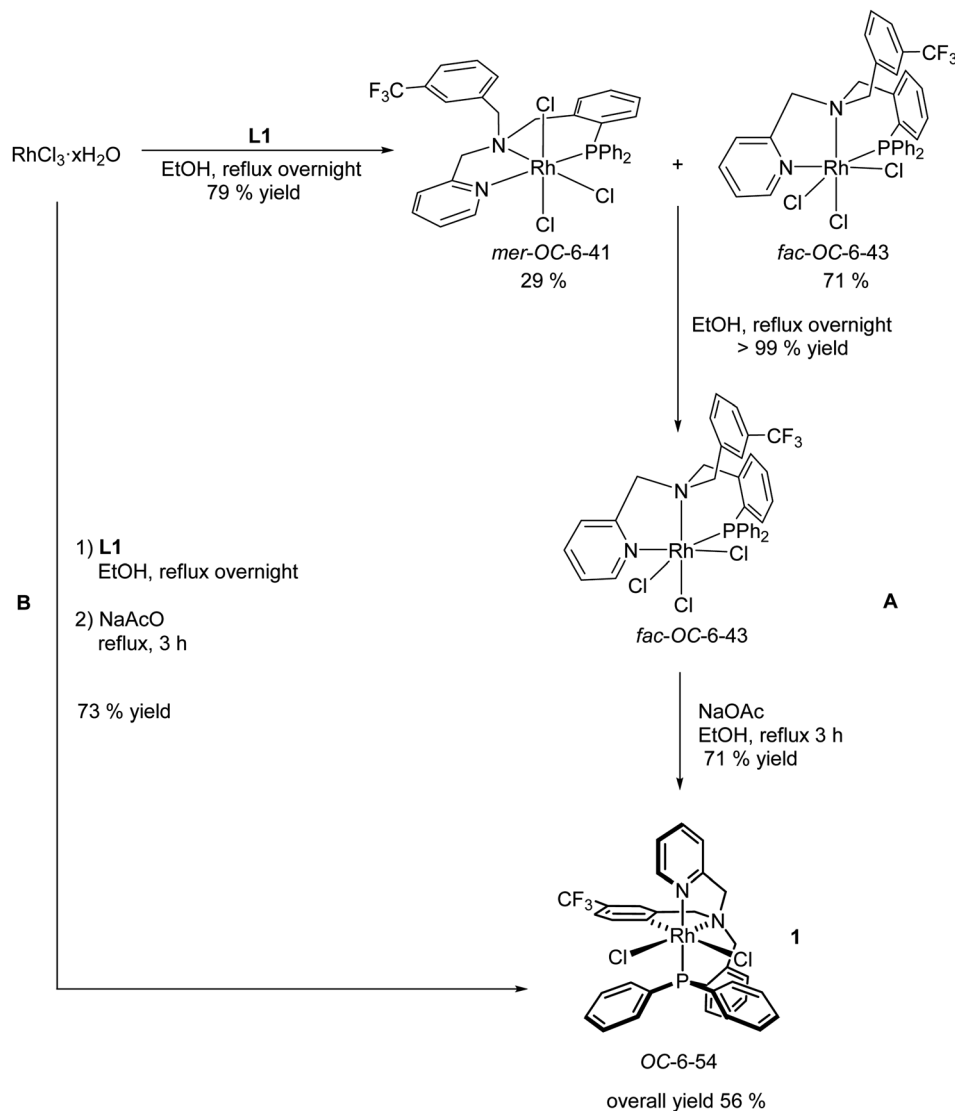
We have developed an improved synthesis of the dichlorido complex **1** following a one-pot, two steps reaction. First, RhCl_3 reacts with **L1** in refluxing EtOH; then, the resulting mixture is heated in the same solvent in the presence of NaOAc for 3 h (protocol B, Scheme 3). Only metalation at C6 carbon of the trifluoro aryl substituent was observed in both preparative routes.^{13e}

Synthesis of the solvate complexes $[\text{Rh}(\kappa^4\text{C},\text{N},\text{N}',\text{P}-\text{L1})(\text{NCMe})_2][\text{SbF}_6]_2$ (**2**) and $[\text{Rh}(\kappa^4\text{C},\text{N},\text{N}',\text{P}-\text{L1})(\text{OH}_2)_2][\text{SbF}_6]_2$ (**3**)

Treatment of the dichlorido complex **1** with AgSbF_6 in acetonitrile or in wet dichloromethane affords the solvate complexes $[\text{Rh}(\kappa^4\text{C},\text{N},\text{N}',\text{P}-\text{L1})(\text{NCMe})_2][\text{SbF}_6]_2$ (**2**) or $[\text{Rh}(\kappa^4\text{C},\text{N},\text{N}',\text{P}-\text{L1})(\text{OH}_2)_2][\text{SbF}_6]_2$ (**3**), respectively (eqn (1)).^{13d}



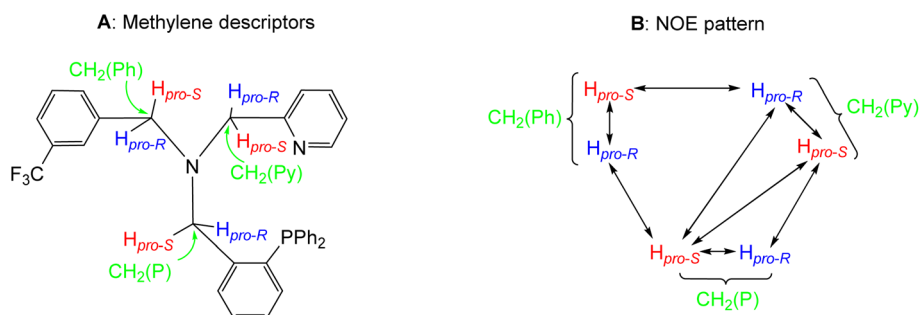
The compounds were characterized by analytical and spectroscopic methods (see Experimental) and by the X-ray determination of the crystal structure of the acetonitrile compound **2**. The metal and the sp^3 nitrogen atoms of the ligand are stereogenic centres. However, the ^1H , $^{31}\text{P}\{^1\text{H}\}$ and $^{13}\text{C}\{^1\text{H}\}$ NMR spectra of complexes **2** and **3** consists of only one set of sharp resonance signals indicating that only one of the three possible isomers^{13e} has been isolated. NMR measurements allow us to ascertain the geometry of the isolated isomer. As the spectroscopy features of both compounds are comparable, we will focus our discussion on the acetonitrile compound **2** as the model. The value of the $J(\text{PH})$ coupling constants together with COSY, HSQC and HMBC experiments permit the assignment of the three pairs of diastereotopic protons which have been labelled



Scheme 3 Synthesis of the dichlorido complex $[\text{RhCl}_2(\kappa^4\text{C},\text{N},\text{N}',\text{P}-\text{L1})]$ as described in the bibliography.^{13e} (A) and as reported in this work (B).

as $\text{CH}_2(\text{Py})$, $\text{CH}_2(\text{Ph})$ and $\text{CH}_2(\text{P})$ (see Scheme 4A). Scheme 4B shows the NOE pattern measured for these six methylene protons. Additionally, the methyl protons of the acetonitrile ligand *trans* to the sp^3 nitrogen atom exhibit NOE relationship with the 6-CH(Py) and 6-CH(Ph) protons of the tetradentate

ligand. Accordingly, a $J(\text{PH})$ coupling constant of 4.0 Hz was measured for the proton-6 of the pyridine moiety (6-CH(Py)). At this point, it should be noted that when the ligand **L1** coordinates with a metal in an octahedral geometry with a $\kappa^4\text{C},\text{N},\text{N}',\text{P}$ coordination mode, the relative configuration of the sp^3



Scheme 4 Assignment of the methylene descriptors (A) and NOE pattern (B) on OC-6-35 isomers of complex 2.



nitrogen atom becomes pre-determined by the configuration at the metal. In particular, in the case of complex **2**, the *A* (*C*) configuration^{14d} at the rhodium atom forces an *R* (*S*) configuration at the sp^3 nitrogen atom. Hence, we propose that compound **2** has been obtained as a racemic mixture of the isomers C_{Rh},S_N and A_{Rh},R_N .^{14,15} as, indeed, it has been corroborated by the X-ray determination of the crystal structure of compound **2**.

A view of the structure of the C_{Rh},S_N isomer of the cation of the complex **2** (ref. 16) is depicted in Fig. 1 and relevant characteristics of the metal coordination sphere are summarized in Table 1. The cation presents an octahedral geometry in which four ligating atoms of **L1** are coordinated in a tripodal fashion and two acetonitrile ligands occupy the two remaining coordination sites arranged *cis* to each other. The phosphorus atom is *trans* to the pyridinic nitrogen N(2), while the nitrile nitrogen atoms N(3) and N(4) are found to be *trans* to the sp^3 nitrogen N(1) and to the aromatic C(28) carbon atoms, respectively. As a reflect of the different *trans* influence the Rh-N(4) bond distance (2.170(4) Å, *trans* to carbon atom) is about 0.142 Å greater than the Rh-N(3) bond distance (2.028(4) Å, *trans* to the sp^3 nitrogen atom). The complex crystallizes in the $P\bar{1}$ space group of the triclinic crystallographic system and, therefore, the unit cell contains two enantiomers of the chiral complex OC-6-35 that, taking into account the arrangement of the coordination atoms around the metal, are the C_{Rh},S_N and A_{Rh},R_N diastereomers. It is important to remark that the relative configuration of the metal is retained when the two chloride ligands are released and exchanged by two solvent molecules. Changes in the notation of the descriptors are due to the application of the nomenclature rules for octahedral complexes.^{14d}

From the point of view of the catalytic applications, an important feature of the chiral complex **2** is the relative disposition of the phenyl groups of the PPh_2 fragment and the two coordinated acetonitrile molecules. As it can be seen in Fig. 2, whereas one face of the plane defined by the two linear acetonitrile molecules is shielded by the phenyl substituents of the

Table 1 Selected bond lengths (Å) and angles (°) of complex **2**

Rh-P	2.2968(12)	N(1)-Rh-N(2)	80.10(15)
Rh-N(1)	2.069(4)	N(1)-Rh-N(3)	174.12(15)
Rh-N(2)	2.102(4)	N(1)-Rh-N(4)	90.59(14)
Rh-N(3)	2.028(4)	N(1)-Rh-C(28)	84.30(16)
Rh-N(4)	2.170(4)	N(2)-Rh-N(3)	94.02(15)
Rh-C(28)	2.007(4)	N(2)-Rh-N(4)	88.84(14)
P-Rh-N(1)	95.17(11)	N(2)-Rh-C(28)	86.84(16)
P-Rh-N(2)	174.91(11)	N(3)-Rh-N(4)	89.56(14)
P-Rh-N(3)	90.69(11)	N(3)-Rh-C(28)	95.16(16)
P-Rh-N(4)	93.15(11)	N(4)-Rh-C(28)	173.81(16)
P-Rh-C(28)	90.81(13)		

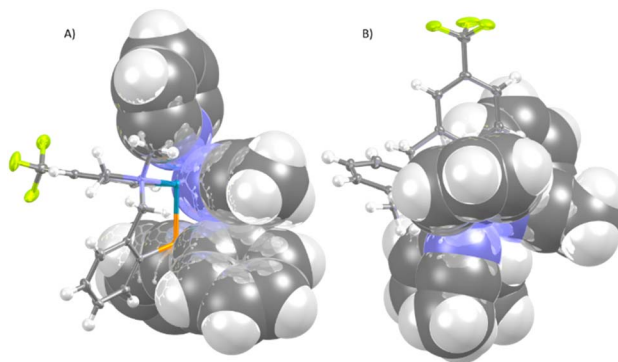


Fig. 2 View of the cation of the complex (S_N)-OC-6-35-C-2 along (A) and perpendicular to (B) the acetonitriles mean plane, showing the phenyl rings shielding.

diphosphino group, the other face is unencumbered. Therefore, when, in complex **2**, prochiral substrates coordinate the metal displacing the labile acetonitrile ligands, the attack of a putative reagent would take preferably through the less hindered enantioface of the substrate originating enantioselectivity in the involved process.

Resolution of the $A_{Rh},R_N/C_{Rh},S_N$ racemate of the solvate complex **2**

As above mentioned, complex **2** was obtained as an equimolar mixture of the C_{Rh},S_N and A_{Rh},R_N diastereomers. In order to apply this complex as an asymmetric catalyst, it is necessary to resolve the obtained racemate. To this end, we developed a diastereomerization protocol of resolution using (*S*)-phenylglycine as a chiral auxiliary.

Reaction of complexes **2 with (*S*)-phenylglycine.** Racemic **2** reacted with enantiopure (*S*)-phenylglycine in refluxing ethanol in the presence of $NaHCO_3$ to afford 1/1 diastereomeric mixtures of (A_{Rh},S_N,S_C)-**4** and (C_{Rh},R_N,S_C)-**4** (eqn (2)).^{14d,15} The new complexes were characterized by spectroscopic and analytical methods (see Experimental). In particular, for both diastereomers, a NOE relationship between the NH_2 protons of the amino carboxylate ligand and one of the protons of each one of the $CH_2(Py)$ and $CH_2(P)$ methylene groups, indicates that the isolated isomers are those in which the oxygen atom of the amino carboxylate group is *trans* to the sp^3 nitrogen of the

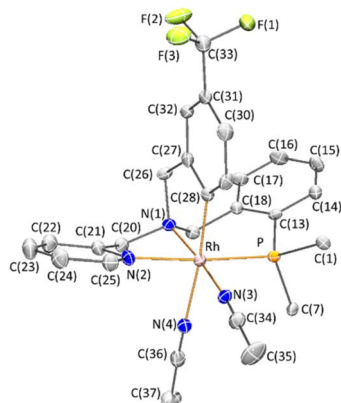
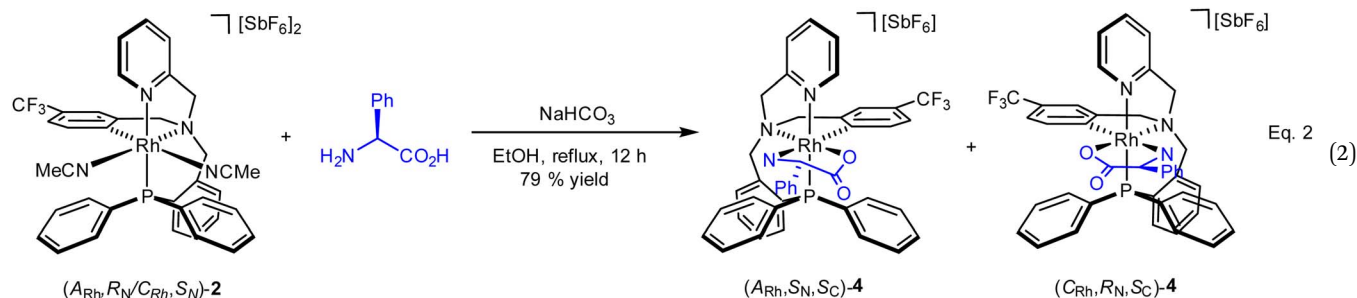


Fig. 1 The crystal structure of racemic cation of **2**. The (S_N)-OC-6-35-C enantiomer of the racemate is depicted. For clarity, hydrogen atoms have been omitted, and only ipso-carbon atoms of phenyl groups are depicted.



tetradentate ligand (eqn (2)). Probably, as it was found by DFT calculations carried out on a phenylglycinato rhodium complex containing a related tripodal tetradentate ligand,^{13c} diastereomers with the oxygen atom *trans* to the sp^3 nitrogen of the tetradentate ligand are more stable than the corresponding isomers in which the oxygen atom is *trans* to the metalated

diastereomers consists of two doublets centred at 29.67 ppm ($J(\text{RhP}) = 130.8$ Hz), assigned to the $(A_{\text{Rh}}, S_{\text{N}}, S_{\text{C}})$ -4 isomer, and at 28.83 ppm ($J(\text{RhP}) = 130.1$ Hz), attributed to the $(C_{\text{Rh}}, R_{\text{N}}, S_{\text{C}})$ -4 isomer (see ESI†). Crystallization of the 1/1 mixture of isomers from MeOH/Et₂O affords a 57/43 molar ratio mixture from which individual diastereomers were separated by chromatography.



carbon atom. Assuming a similar behaviour for complex 2, stereoselection in the formation of the isolated glycinate complexes 4 would mainly rely on thermodynamics.

The determination of the absolute configuration of each of the complexes has been carried out by NMR from a mixed solution of the two diastereomers (see ESI†). In particular, the 6-CH(Py) proton ($\delta = 8.32$ ppm) of one diastereomer exhibits a nuclear Overhauser effect (NOE) with the asymmetric C*H proton ($\delta = 3.98$ ppm) determining the configuration for this diastereomer as $(A_{\text{Rh}}, S_{\text{N}}, S_{\text{C}})$ -4. In the other diastereomer, determined as $(C_{\text{Rh}}, R_{\text{N}}, S_{\text{C}})$ -4, the C*H proton ($\delta = 3.10$ ppm) correlates by NOE with the phenyl protons of the PPh₂ fragment ($\delta = 7.74$ ppm). The $^{31}\text{P}\{^1\text{H}\}$ NMR spectrum of the mixture of

Separation of the diastereomeric mixture of glycinate complexes. Diastereomeric mixtures of $(A_{\text{Rh}}, S_{\text{N}}, S_{\text{C}})$ -4 and $(C_{\text{Rh}}, R_{\text{N}}, S_{\text{C}})$ -4 were separated by flash chromatography on a silica column using a CH₂Cl₂/MeOH mixture as eluent (see Experimental). Three fractions A, B and C were consecutively collected. Fraction A (ca. 21% yield) was diastereopure $(A_{\text{Rh}}, S_{\text{N}}, S_{\text{C}})$ -4. Fraction B (ca. 48% yield) was a mixture of the two diastereomers $(A_{\text{Rh}}, S_{\text{N}}, S_{\text{C}})$ -4 and $(C_{\text{Rh}}, R_{\text{N}}, S_{\text{C}})$ -4 that was recycled. Fraction C (ca. 18% yield) was diastereopure $(C_{\text{Rh}}, R_{\text{N}}, S_{\text{C}})$ -4.

The $^{31}\text{P}\{^1\text{H}\}$ NMR spectrum of the starting mixture and those of each diastereomer, once separated by chromatography, are shown in Fig. 3.

Replacement of the coordinated auxiliary. The chiral auxiliary was replaced with two chlorido ligands, under retention of the configuration, by addition of excess of concentrated HCl(aq). From diastereopure $(A_{\text{Rh}}, S_{\text{N}}, S_{\text{C}})$ - and $(C_{\text{Rh}}, R_{\text{N}}, S_{\text{C}})$ -4, enantiopure dichlorido $(A_{\text{Rh}}, R_{\text{N}})$ -1 and $(C_{\text{Rh}}, S_{\text{N}})$ -1 were obtained, respectively, in more than 99.5/0.5 enantiomeric ratio in both cases.¹⁷ Fig. 4 shows the HPLC traces of a racemic mixture of the dichlorido complex 1 as well as those of the pure enantiomers $(C_{\text{Rh}}, S_{\text{N}})$ -1 and $(A_{\text{Rh}}, R_{\text{N}})$ -1. The circular dichroism spectra of both enantiomers are shown in Fig. 4, too. No significant changes of the HPLC traces were observed when enantiopure 1 was heated at 80 °C in methanol, in a high-pressure NMR tube, for 48 h. Thus, it can be argued that the configuration at the metal is thermally stable.

From the enantiopure chlorido complex $(A_{\text{Rh}}, R_{\text{N}})$ -1, enantiopure solvate complex $(A_{\text{Rh}}, R_{\text{N}})$ -2 was obtained following the treatment above reported for the preparation of racemic solvate complexes from racemic chlorido complex 1 (eqn (1)).

Catalytic Diels–Alder reaction between methacrolein and cyclopentadiene

Complexes 2 and 3 catalyze the Diels–Alder reaction between methacrolein (MA) and cyclopentadiene (HCP) in

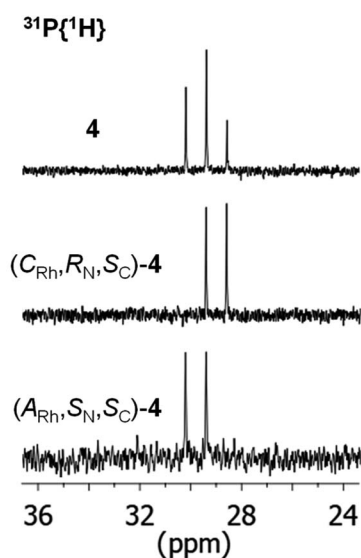
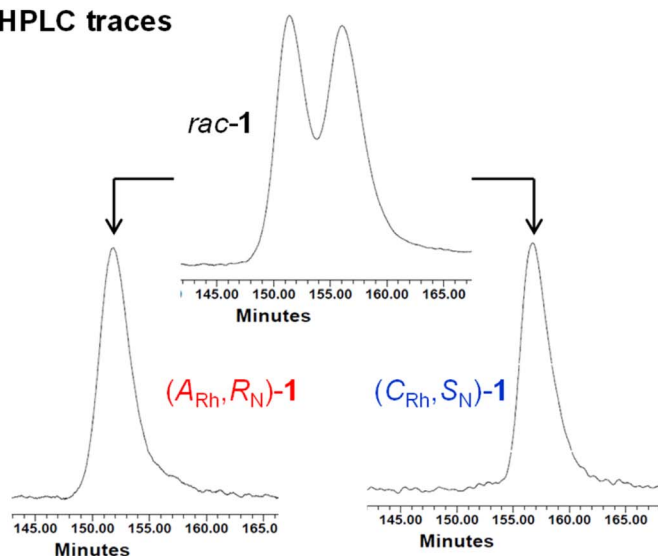


Fig. 3 $^{31}\text{P}\{^1\text{H}\}$ NMR of the starting mixture of complexes 4 (above) and the individual diastereomers $(C_{\text{Rh}}, R_{\text{N}}, S_{\text{C}})$ -4 (middle) and $(A_{\text{Rh}}, S_{\text{N}}, S_{\text{C}})$ -4 (below).



HPLC traces



CD spectra

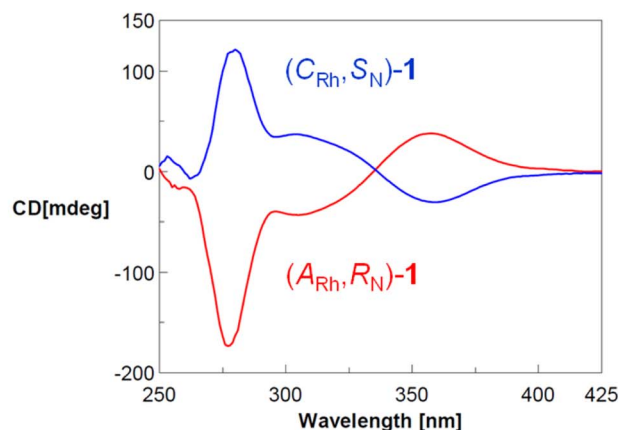


Fig. 4 HPLC traces of *rac*-1, (*A*_{Rh},*R*_N)-1 and (*C*_{Rh},*S*_N)-1 and CD spectra of (*A*_{Rh},*R*_N)-1 (red) and (*C*_{Rh},*S*_N)-1 (blue).

Table 2 Selected data for the reaction between MA and HCp catalyzed by the complexes 2 and 3^a

Entry	Cat.	Cat. loading (mol%)	<i>T</i> (K)	<i>t</i> (h)	Conv. ^b (%)	<i>exo/endo</i>	er ^{c,d} (<i>R/S</i>)
1	(<i>rac</i>)-2	10	298	6	92	95/5	—
2	(<i>rac</i>)-2	5	298	15	86	98/2	—
3	(<i>rac</i>)-2	10	273	24	82	83/17	—
4	(<i>rac</i>)-2	10	263	140	61	88/12	—
5	(<i>rac</i>)-3	10	298	12	90	94/6	—
6	(<i>rac</i>)-3	5	298	24	87	96/4	—
7	(<i>A</i> _{Rh} , <i>R</i> _N)-2	10	298	8	97	93/7	>99/1

^a Reaction conditions: catalyst, 1.16×10^{-3} or 2.32×10^{-3} mmol (5 or 10 mol%); MA, 23.0×10^{-3} mmol; HCp, 81.0×10^{-3} mmol and 10 mg of 4 Å MS, in 0.5 mL of CD₂Cl₂. ^b Based on MA. ^c Determined by ¹H NMR. ^d Determined for the *exo* isomer by integration of the ¹H NMR signals in presence of the chiral shift reagent (+)-Eu(hfc)₃. ^e Absolute configuration of the major *exo* adduct (*R* at C2) was established by comparison of the aldehyde proton splitting in presence of (+)-Eu(hfc)₃ with previous work indicating the relative splitting of the (*R*)-*exo* and (*S*)-*exo* adducts.¹⁸

dichloromethane. To determine the optimal conditions, we first tested the activity of *rac*-2 and *rac*-3. As shown in Table 2, at 298 K, to get good conversions with a catalyst loading of 5 or 10 mol%, several hours are needed (entries 1, 2, 5 and 6). Decreasing temperature increases the reaction time and diminishes the obtained *exo/endo* ratio of the adduct (entries 3 and 4). Complex 2 is more active than complex 3 (compare entries 1 and 2 with entries 5 and 6, respectively). At 5 mol% of catalyst loading, better *exo/endo* ratios than at 10 mol% catalyst loading were achieved but, to reach similar conversions, it is necessary to increase importantly the reaction time (entries 1, 2 and 5, 6). Taking into account all these data, we carried out the reaction between methacrolein and cyclopentadiene using 10 mol% of enantiopure (*A*_{Rh},*R*_N)-2, at 298 K. After 8 h of reaction, 97% of conversion was achieved with an *exo/endo* ratio of 93/7. Notably, enantioselectivity in the *R* at C2 isomer almost perfect was obtained (er > 99/1, entry 7). Comparing the catalytic

results using the CF₃-substituted (*A*_{Rh},*R*_N)-2 complex with those of the unsubstituted one^{13c} (after 24 h at 298 K, conv. 93%; *exo/endo* ratio: 88/12; er: 91/9), the CF₃-substituted complex has about 3 times higher catalytic activity, better diastereoselectivity and a remarkable increase in enantioselectivity, from 91/9 to >99/1 of er. These catalytic differences are understood by a large difference in the *trans* effect favourable to the CF₃ group which enhances the catalytic activity by favouring the de-and coordination of the substrates. On the other hand, enantioselectivity increases because the non-catalytic route to products becomes less competitive *versus* the catalytic route.

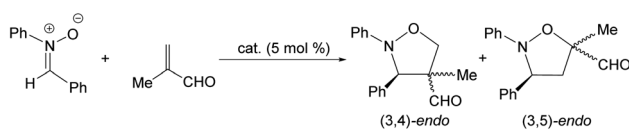
Catalytic 1,3-dipolar cycloaddition reaction between methacrolein and *N*-benzylidenphenylamine-*N*-oxide

Complex 2 also catalyzes the 1,3-dipolar cycloaddition reaction between methacrolein and the nitron *N*-



benzylidenphenylamine-*N*-oxide. Table 3 lists a selection of the results obtained together with the reaction conditions employed. First, we tested *rac*-2 as the catalyst (entries 1–4). To achieve moderate to good conversions, 24 h of reaction are necessary even operating at 298 K (entry 1). Only *endo* isomers were detected and good regioselectivity in favour of the 3,5-*endo* isomer was obtained under all conditions explored. At 298 K, using (*A*_{Rh},*R*_N)-2 as the catalyst, an enantiomeric ratio of 94/6 was measured for the major adduct of the 3,5-*endo* diastereomer (entry 5). Lowering temperature to 273 K diminishes the er from 94/6 to 84/16 (entry 6). As long reaction times are necessary to reach acceptable conversions, a greater contribution of the thermal reaction is, probably, at the origin of the observed lowering of the er.

Table 3 Selected data for the reaction between MA and *N*-benzylidenphenylamine-*N*-oxide catalyzed by complex 2^a



Entry	Cat.	<i>T</i> (K)	<i>t</i> (h)	Conv. ^b (%)	(3,4)/(3,5) ^c	er ^d
1	(<i>rac</i>)-2	298	24	64	5/95	—
2	(<i>rac</i>)-2	281	24	17	2/98	—
3	(<i>rac</i>)-2	273	24	8	6/94	—
4	(<i>rac</i>)-2	263	24	0	—	—
5	(<i>A</i> _{Rh} , <i>R</i> _N)-2	298	24	78	4/96	94/6
6	(<i>A</i> _{Rh} , <i>R</i> _N)-2	273	164	68	12/88	84/16

^a Reaction conditions: catalyst 1.16×10^{-3} mmol (5.0 mol%); MA 70.0×10^{-3} mmol, 10 mg of 4 Å MS, and nitron 35.0×10^{-3} mmol in 0.5 mL of CD₂Cl₂. ^b Based on nitron. Determined by ¹H NMR. ^c Only *endo* isomers were detected. ^d Determined for the 3,5-*endo* isomer by integration of the ¹H NMR signals of the diastereomeric (*S*)-methylbenzylimine derivatives.¹⁹

Proposed mechanism and origin of the enantioselectivity

The proposed catalytic cycle is depicted in Fig. 5A. One molecule of methacrolein (MA) replaces the more labile molecule of acetonitrile *trans* to the aromatic carbon atom of the enantiopure catalyst (*A*_{Rh},*R*_N)-2. Assuming that the methacrolein coordinates as a planar molecule with an *s-trans* conformation for the double carbon–oxygen and carbon–carbon bonds and with an *E*-configuration around the carbon–oxygen double bond,²⁰ its Si-face becomes much more accessible to the cyclopentadiene or to the nitron than its Re-face, because, in the chiral pocket generated in the diastereopure catalyst, the Re-face is shielded by the phenyl rings of the PPh₂ group (Fig. 5B). An attack of the cyclopentadiene substrate through the Si-face of the methacrolein renders the *R* at C2 enantiomer of the DA adduct as it was experimentally observed. On the other hand, an *endo* approach of the nitron through the Si-face of the coordinated methacrolein would render the 3*R*,5*R* isomer of the corresponding isoxazolidine.

Conclusions

Judiciously designed achiral tripodal tetradentate ligands are able to generate octahedral rhodium complexes in which the metal is a stereogenic centre. This is the case of the dichlorido complex 1. The frame generated by the polydentate ligand confers configurational stability to the octahedral molecule even when the two remaining positions are occupied by labile solvent molecules as in complexes 2 and 3. Notably, the compounds 2 and 3 meet two important requirements that make them good candidates for asymmetric catalysts: configurational stability and labile coordination positions. Indeed, after stereochemical resolution the chiral complex (*A*_{Rh},*R*_N)-2 catalyzes the Diels–Alder reaction between methacrolein and cyclopentadiene with a >99/1 enantiomeric ratio. Furthermore, the same catalyst mediates the 1,3-dipolar cycloaddition reaction between methacrolein and the nitron

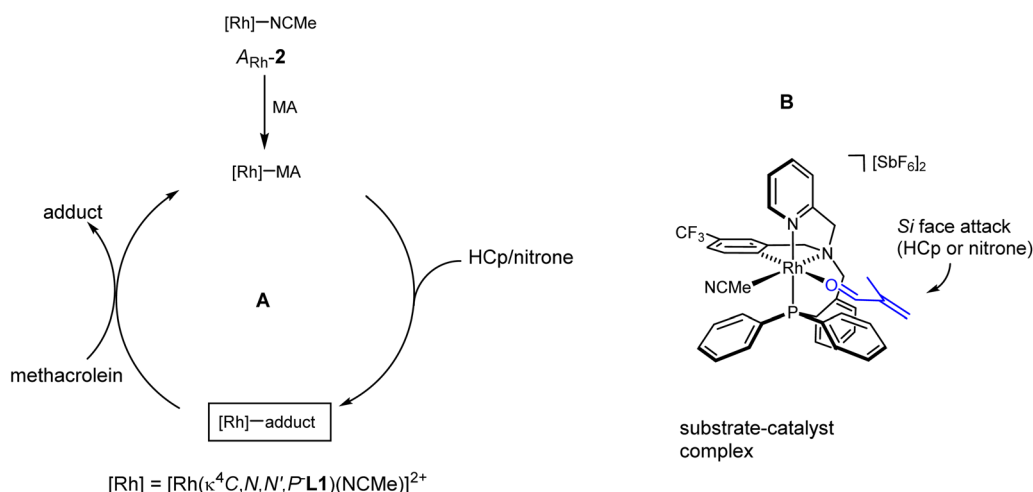


Fig. 5 Proposed catalytic cycle (A) and the suggested model for the asymmetric induction (B).



N-benzylidenphenylamine-*N*-oxide affording only *endo*-adducts with enantiomeric ratios of up to 94/6 for the 3,5-*endo* adduct. The molecular structure of complex **2**, determined by X-ray diffraction analysis, reveals the presence of a chiral pocket around the labile solvent molecules coordination sites. When a prochiral substrate coordinates the metal inside this chiral pocket, the two phenyl groups of the tetradentate ligand shield one of its enantiofaces. Consequently, an incoming reagent preferentially approaches the coordinated substrate through its clearer enantioface resulting in enantioselection.

Finally, the findings reported in this work open the door to the design and use of new polydentate ligands capable of generating stereogenic metal centres both in octahedral metal geometries and in metal complexes with other coordination numbers. Likewise, the studies can be extended to other metals and, in particular, to cheap, non-toxic and earth-abundant metals of the first transition series, with inherent economic and environmental benefits. Further work in this area is in progress in our laboratory and will be reported in due course.

Experimental

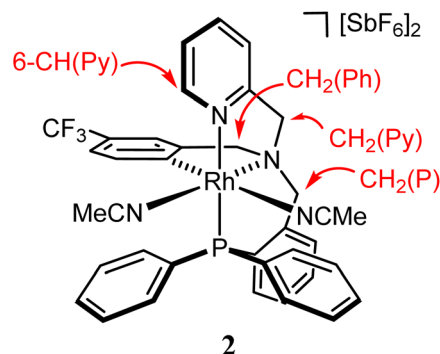
All preparations have been carried out under argon, unless otherwise stated. All solvents were treated in a PS-400-6 Innovative Technologies Solvent Purification System (SPS). Infrared spectra were recorded on PerkinElmer Spectrum-100 (ATR mode) FT-IR spectrometer. CD spectra were determined in MeOH (*ca.* 4×10^{-4} mol L⁻¹ solutions) in a 1 cm path length cell by using a Jasco-810 apparatus. Carbon, hydrogen and nitrogen analyses were performed using a PerkinElmer 240 B microanalyzer. ¹H, ¹³C and ³¹P spectra were recorded on a Bruker AV-300 (300.13 MHz), a Bruker AV-400 (400.16 MHz) or a Bruker AV500 (500.13 MHz) spectrometers. Chemical shifts are expressed in ppm upfield from SiMe₄, 85% H₃PO₄ (³¹P) or CFCl₃ (¹⁹F). COSY, NOESY, HSQC, HMQC, and HMBC ¹H-X (X = ¹H, ¹³C, ³¹P) correlation spectra were obtained using standard procedures. Flash chromatography was performed on an Interchim (PuriFlash 450) instrument using a PF-50SIHP column (25 g, 30 μm).

Improved synthesis of the complex **1**

At RT, to a suspension of RhCl₃ × H₂O (1.00 g, 3.85 mmol) in 20 mL of ethanol, 2.07 g of **L1** were added. The resulting suspension was stirred under reflux overnight. During this time, the colour of the suspension gradually changes from pink-red to yellow. After the reaction time, the suspension was cooled to room temperature and 2.21 g (8.31 mmol) of NaAcO was added. The resulting suspension was stirred for 3 h under reflux. During this time, a yellow precipitate was formed. The solid was filtered off and extracted with CH₂Cl₂ (3 × 15 mL). The resulting

yellow solution was vacuum-dried to give analytically pure compound **1**. Yield: 2.01 g (73%). The spectroscopic data for complex **1** were in agreement with the previously reported in the literature.^{13e}

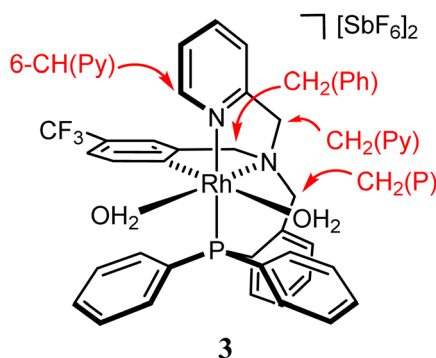
Preparation and characterization of the complex **2**



To a solution of [RhCl₂(κ⁴C,N,N',P-L1)] (**1**) (1.00 g, 1.40 mmol) in 40 mL of acetonitrile, 963.4 mg (2.81 mmol) of AgSbF₆ were added. The resulting suspension was placed under reflux for 40 h and then filtered to remove any insoluble material. The resulting light yellow solution was evaporated to *ca.* 1 mL. The slow addition of Et₂O (25 mL) led to the precipitation of a pale yellow solid that was filtered off, washed with Et₂O (3 × 5 mL) and vacuum-dried. Yield: 1.54 g (92%) Anal. calcd C₃₇H₃₃F₁₅N₄PRhSb₂·2CH₂Cl₂: C, 34.30; H, 2.73; N, 4.10. Found: C, 34.13; H, 2.67; N, 3.97. IR (solid, cm⁻¹): ν(CN) 2327 (br), ν(CN) 2298 (br), ν(SbF₆) 654 (s). ¹H NMR (500.13 MHz, CD₂Cl₂/acetone-d₆, RT, ppm): δ = 8.50 (broad pseudo-triplet, *J* = 4.6 Hz, 1H, 6-CH(Py)), 8.01 (ptd, *J* = 7.8, 1.4 Hz, 1H, CH(Ar)), 7.80–7.42 (m, 14H, H(Ar)), 6.97 (d, *J* = 9.6 Hz, 1H, 5-CH(Ph)), 6.84–6.78 (m, 4H, 2 × CH(Ar), 6-CH(Ph), 3-CH(Ph)), 5.22 (d, *J* = 15.8 Hz, 1H, pro-S-CH₂(Py)), 4.75 (d, *J* = 16.0 Hz, 1H, pro-R-CH₂(P)), 4.74 (d, *J* = 14.0 Hz, 1H, pro-R-CH₂(Py)), 4.64 (d, *J* = 17.9 Hz, 1H, pro-R-CH₂(Ph)), 4.52 (ddd, *J* = 14.1, 5.0, 1.8 Hz, 1H, pro-S-CH₂(P)), 4.07 (d, *J* = 17.9 Hz, 1H, pro-S-CH₂(Ph)), 2.69 (s, 3H, NCMe *cis* to C), and 2.42 (s, 3H, NCMe *trans* to C). ¹³C{¹H} NMR (125.77 MHz, CD₂Cl₂/acetone-d₆, RT, ppm): δ = 155.79 (d, *J* = 1.9 Hz, 2-C(Py)), 149.30 (brdd, *J*_{Rh-C} = 29.1 Hz, *J*_{P-C} = 8.7 Hz, CRh), 148.30 (s, 6-CH(Py)), 148.16 (s, 2-C(Ph)), 141.05–128.45 (m, 18C(H)(Ar)), 127.30 (q, *J*_{Rh-C} = 32.4 Hz, 4-C(Ph)), 127.08 (d, *J*_{Rh-C} = 5.8 Hz, NCMe *cis* to C), 123.52 (q, *J*_{F-C} = 271.40 Hz, CF₃), 125.98–120.26 (m, 6C(H)(Ar)), 124.13 (brs, NCMe *trans* to C), 74.31 (s, CH₂(Py)), 66.95 (d, *J* = 7.9 Hz, CH₂(P)), 66.24 (s, CH₂(Ph)), 3.95 (s, NCMe *cis* to C), 1.08 (s, NCMe *trans* to C). ¹⁹F{¹H} NMR (282.33 MHz, CD₂Cl₂/acetone-d₆, RT, ppm): δ = -65.52 (s). ³¹P{¹H} NMR (202.46 MHz, CD₂Cl₂/acetone-d₆, RT, ppm): δ = 28.58 (d, *J* = 114.1 Hz).



Preparation and characterization of the complex 3

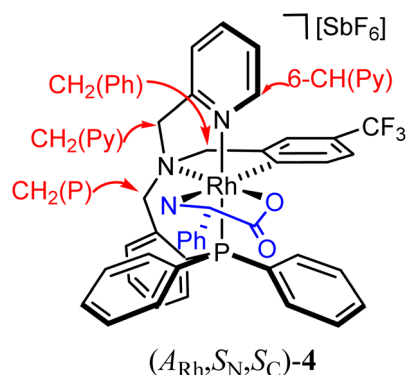


At room temperature, to a solution of $[\text{RhCl}_2(\kappa^4\text{C},\text{N},\text{N}',\text{P}-\text{L1})]$ (**1**) (500.0 mg, 0.701 mmol) in 30 mL of wet dichloromethane, 1.55 mmol of AgSbF_6 were added. The pale yellow suspension was stirred for 72 h and then was filtered to remove the AgCl formed. The solution was evaporated to *ca.* 5 mL. Addition of 10 mL Et_2O and 10 mL of *n*-pentane led to the precipitation of a light yellow solid that was filtered off and vacuum-dried to afford complex **3** as a microcrystalline solid. Yield: 460.0 mg (57%). Anal. calcd $\text{C}_{33}\text{H}_{31}\text{F}_{15}\text{N}_2\text{O}_2\text{PRhSb}_2$: C, 34.47; H, 2.72; N, 2.44. Found: C, 34.16; H, 2.57; N, 2.51. IR (solid, cm^{-1}): $\nu(\text{OH})$ 3500 (br), $\nu(\text{SbF}_6)$ 653 (s). ^1H NMR (500.13 MHz, CD_2Cl_2 , RT, ppm): δ = 8.32 (pt, J = 4.2 Hz, 1H, 6-CH(Py)), 7.96–6.66 (m, 20H, H(Ar)), 4.98 (d, J = 16 Hz, 1H, pro-*S*- $\text{CH}_2(\text{Py})$), 4.74–4.67 (overlapped, 4H, 2 \times OH_2), 4.59 (d, J = 14.4 Hz, 1H, pro-*R*- $\text{CH}_2(\text{P})$), 4.53 (d, J = 15.6 Hz, 1H, pro-*R*- $\text{CH}_2(\text{Py})$), 4.49 (d, J = 18.5 Hz, 1H, pro-*R*- $\text{CH}_2(\text{Ph})$), 4.30 (dd, J = 14.8, 3.2 Hz, 1H, pro-*S*- $\text{CH}_2(\text{P})$), 3.94 (d, J = 18.2 Hz, 1H, pro-*S*- $\text{CH}_2(\text{Ph})$). $^{13}\text{C}\{^1\text{H}\}$ NMR (125.77 MHz, CD_2Cl_2 , RT, ppm): δ = 155.87 (s, 2-C(Py)), 147.97 (s, 2-C(Ph)), 147.55 (s, 6-CH(Py)), 143.20 (dd, $J_{\text{Rh-C}} = 32.2$ Hz, $J_{\text{P-C}} = 12.5$ Hz, 1H, CRh), 141.74–116.54 (m, 21C(H)(Ar)), 111.63 (q, $J_{\text{F-C}} = 300.7$ Hz, CF_3), 73.81 (s, $\text{CH}_2(\text{Py})$), 66.78 (d, J = 7.4 Hz, $\text{CH}_2(\text{P})$), 66.30 (s, $\text{CH}_2(\text{Ph})$). $^{19}\text{F}\{^1\text{H}\}$ NMR (282.33 MHz, CD_2Cl_2 , RT, ppm): δ = –62.79 (s). $^{31}\text{P}\{^1\text{H}\}$ NMR (202.46 MHz, CD_2Cl_2 , RT, ppm): δ = 27.74 (d, J = 125.6 Hz).

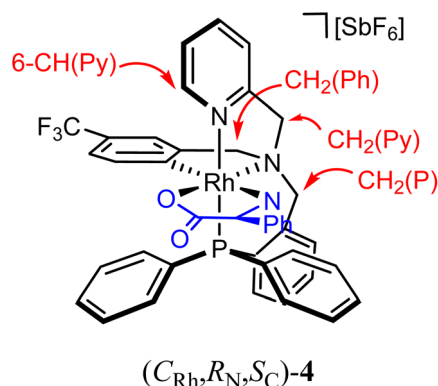
Preparation and characterization of the diastereomers ($\text{C}_{\text{Rh}},\text{R}_{\text{N}},\text{S}_{\text{C}}/\text{A}_{\text{Rh}},\text{S}_{\text{N}},\text{S}_{\text{C}}$)-4

To a suspension of 72.1 mg (0.477 mmol) of (*S*)-phenylglycine in 40 mL of EtOH , 60.1 mg (0.715 mmol) of NaHCO_3 were added. After 15 min of vigorous stirring, 600.0 mg (0.502 mmol) of $\text{rac}[\text{Rh}(\kappa^4\text{C},\text{N},\text{N}',\text{P}-\text{L1})(\text{NCMe})_2][\text{SbF}_6]_2$ (**2**) were added and the resulting suspension was refluxed for 12 h. After cooling the reaction mixture to RT, the solvent was vacuum-evaporated until dryness and the residue was extracted with CH_2Cl_2 (4 \times 15 mL). The resulting solution was vacuum-concentrated until *ca.* 3 mL. The addition of Et_2O afforded a pale yellow solid which was filtered off, washed with Et_2O (2 \times 3 mL) and dried under vacuum. Yield: 406.2 mg (79%). Molar ratio ($\text{C}_{\text{Rh}},\text{R}_{\text{N}},\text{S}_{\text{C}}$)-4:($\text{A}_{\text{Rh}},\text{S}_{\text{N}},\text{S}_{\text{C}}$)-4, 1/1. Crystallization of

this mixture from $\text{MeOH}/\text{Et}_2\text{O}$ affords a ($\text{C}_{\text{Rh}},\text{R}_{\text{N}},\text{S}_{\text{C}}$)-4/($\text{A}_{\text{Rh}},\text{S}_{\text{N}},\text{S}_{\text{C}}$)-4, 57/43 molar ratio mixture of diastereomers. Anal. calcd $\text{C}_{41}\text{H}_{35}\text{F}_9\text{N}_3\text{O}_2\text{PRhSb}$: C, 49.77; H, 3.56; N, 4.24. Found: C, 49.38; H, 3.47; N, 4.00. IR (solid, cm^{-1}): $\nu(\text{NH}_2)$ 2959 (br), $\nu(\text{C}=\text{O})$ 1640 (s), $\nu(\text{SbF}_6)$ 656 (s).



($\text{A}_{\text{Rh}},\text{S}_{\text{N}},\text{S}_{\text{C}}$)-4 diastereomer. ^1H NMR (500.13 MHz, CD_2Cl_2 , RT, ppm): δ = 8.32 (broad pseudo-triplet, J = 4.0 Hz, 1H, 6-CH(Py)), 7.96–6.60 (m, 25H, CH(Ar)), 5.28 (d, J = 15.6 Hz, 1H, pro-*S*- $\text{CH}_2(\text{Py})$), 5.02 (dd, J = 11.0, 6.3 Hz, 1H, pro-*S*- NH_2), 4.94 (d, J = 14.6 Hz, 1H, pro-*S*- $\text{CH}_2(\text{P})$), 4.67 (d, J = 15.9 Hz, 1H, pro-*R*- $\text{CH}_2(\text{Py})$), 4.60–4.54 (m, 2H, pro-*S*- $\text{CH}_2(\text{P})$, pro-*R*- $\text{CH}_2(\text{Ph})$), 3.87 (d, J = 17.4 Hz, 1H, pro-*R*- $\text{CH}_2(\text{Ph})$), 3.98 (dd, J = 12.1, 6.3 Hz, 1H, C^*H), 2.79 (pt, J = 11.2 Hz, 1H, pro-*R*- NH_2). $^{13}\text{C}\{^1\text{H}\}$ NMR (125.77 MHz, CD_2Cl_2 , RT, ppm): δ = 179.45 (s, COO), 160.93 (dd, $J_{\text{Rh-C}} = 25.80$ Hz, $J_{\text{P-C}} = 9.90$ Hz, 1H, CRh), 156.11 (d, J = 1.7 Hz, 2 C(Py)), 147.38 (s, 6-CH(Py)), 145.45–115.98 (m, 34C(H)(Ar)), 74.72 (s, $\text{CH}_2(\text{Py})$), 68.65 (d, J = 5.6 Hz, $\text{CH}_2(\text{P})$), 67.26 (s, $\text{CH}_2(\text{Ph})$), 60.05 (s, C^*). $^{19}\text{F}\{^1\text{H}\}$ NMR (282.33 MHz, CD_2Cl_2 , RT, ppm): δ = –62.48 (s). $^{31}\text{P}\{^1\text{H}\}$ NMR (202.46 MHz, CD_2Cl_2 , RT, ppm): δ = 29.67 (d, J = 130.8 Hz).



($\text{C}_{\text{Rh}},\text{R}_{\text{N}},\text{S}_{\text{C}}$)-4 diastereomer. ^1H NMR (500.13 MHz, CD_2Cl_2 , RT, ppm): δ = 8.38 (broad pseudo-triplet, J = 3.9 Hz, 1H, 6-CH(Py)), 7.88–6.61 (m, 25H, CH(Ar)), 5.11 (d, J = 14.8 Hz, 1H, pro-*R*- $\text{CH}_2(\text{P})$), 5.07 (d, J = 15.9 Hz, 1H, pro-*S*- $\text{CH}_2(\text{Py})$), 4.49 (d, J = 16.0 Hz, 1H, pro-*R*- $\text{CH}_2(\text{Py})$), 4.64–4.53 (m, 3H, pro-*S*- $\text{CH}_2(\text{Py})$, pro-*S*- $\text{CH}_2(\text{P})$, pro-*R*- $\text{CH}_2(\text{Ph})$), 4.20 (dd, J = 11.5, 9.3 Hz, 1H, pro-*R*- NH_2), 3.87 (dd, J = 17.4 Hz, 1H, pro-*S*- $\text{CH}_2(\text{Ph})$), 3.71 (dd, J = 12.0, 7.3 Hz, 1H, pro-*S*- NH_2), 3.10 (pt, J = 8.0 Hz, 1H, C^*H). $^{13}\text{C}\{^1\text{H}\}$ NMR (125.77 MHz, CD_2Cl_2 , RT, ppm): δ = 180.06 (s, COO), 160.68 (dd, $J_{\text{Rh-C}} = 24.29$ Hz, $J_{\text{P-C}} = 10.56$ Hz, 1H, CRh), 155.88



(d, $J = 2.0$ Hz, 2-C(Py)), 147.42 (s, 6-CH(Py)), 145.10–115.88 (m, $^{13}\text{C}(\text{H})(\text{Ar})$), 74.84 (s, $\text{CH}_2(\text{Py})$), 68.52 (d, $J = 5.6$ Hz, $\text{CH}_2(\text{P})$), 67.69 (s, $\text{CH}_2(\text{Ph})$), 58.61 (s, C*). $^{19}\text{F}\{^1\text{H}\}$ NMR (282.33 MHz, CD_2Cl_2 , RT, ppm): $\delta = -62.54$ (s). $^{31}\text{P}\{^1\text{H}\}$ NMR (202.46 MHz, CD_2Cl_2 , RT, ppm): $\delta = 28.83$ (d, $J = 130.1$ Hz).

Chromatographic separation of the diastereomers ($C_{\text{Rh}}, R_{\text{N}}, S_{\text{C}}/A_{\text{Rh}}, S_{\text{N}}, S_{\text{C}}$)-4

An equimolar mixture of diastereomers ($C_{\text{Rh}}, R_{\text{N}}, S_{\text{C}}/A_{\text{Rh}}, S_{\text{N}}, S_{\text{C}}$)-[Rh($\kappa^4\text{C}, \text{N}, \text{N}', \text{P-L1}$)]((*S*)-phenylglycinato)][SbF₆] (200.0 mg, 0.194 mmol) was eluted with a $\text{CH}_2\text{Cl}_2/\text{MeOH}$ (98.75/1.25, v/v, 30 mL min⁻¹) mixture on a silica column (SI-HP, 25 g, 30 μm). Three fractions A, B and C, were consecutively collected. Fraction A (43.0 mg, 0.042 mmol, 21%) was diastereopure ($A_{\text{Rh}}, S_{\text{N}}, S_{\text{C}}$)-4. Fraction B (96.0 mg, 0.093 mmol, 48%) was an equimolar mixture of the diastereomers ($C_{\text{Rh}}, R_{\text{N}}, S_{\text{C}}/A_{\text{Rh}}, S_{\text{N}}, S_{\text{C}}$)-4. Fraction C (36.0 mg, 0.035 mmol, 18%) was diastereopure ($C_{\text{Rh}}, R_{\text{N}}, S_{\text{C}}$)-4.

Elimination of the auxiliary. Crystallization of enantiopure ($A_{\text{Rh}}, R_{\text{N}}$)-1 and ($C_{\text{Rh}}, S_{\text{N}}$)-1

To a suspension of diastereopure ($A_{\text{Rh}}, S_{\text{N}}, S_{\text{C}}$)-4 (20.0 mg, 0.019 mmol) in 4 mL of EtOH, 0.20 mL of 12 M HCl(aq) were added. After 48 h at RT, a pale yellow microcrystalline solid precipitated from the bright yellow solution. It was collected by filtration and successively washed with EtOH (3 \times 3 mL) and Et₂O (3 \times 3 mL). The second fraction of the product was obtained from the filtrate (12 mg). Total yield: 89%. The isolated solid was characterized as ($A_{\text{Rh}}, R_{\text{N}}$)-1. The diastereomer ($C_{\text{Rh}}, S_{\text{N}}$)-1 was similarly obtained starting from ($C_{\text{Rh}}, R_{\text{N}}, S_{\text{C}}$)-4 (yield: 87%). The optical purity of the samples was determined by HPLC with a Chiralpak IB column (0.46 \times 25 cm) with IB guard (0.46 cm \times 5 cm) (65/35, $\text{CH}_3\text{CN}/\text{H}_2\text{O}$, 0.1% CF₃COOH; 0.4 mL min⁻¹; t_{R} 151.8 and 156.7 min for ($A_{\text{Rh}}, R_{\text{N}}$)-1 and ($C_{\text{Rh}}, S_{\text{N}}$)-1, respectively). Circular dichroism spectra: ($A_{\text{Rh}}, R_{\text{N}}$)-1 (MeOH, 5.8×10^{-4} M, RT, $\lambda(\text{nm})$ ($\Delta\epsilon$): 282 (−90.96), 205 (−25.28), 360 (+17.68). ($C_{\text{Rh}}, S_{\text{N}}$)-1 (MeOH, 4.0×10^{-4} M, RT, $\lambda(\text{nm})$ ($\Delta\epsilon$): 282 (+106.12), 205 (+26.53), 360 (−11.37).

Preparation of the diastereopure solvate complex 2

Diastereopure ($A_{\text{Rh}}, R_{\text{N}}$)-2 was prepared starting from the corresponding diastereopure chlorido complex ($A_{\text{Rh}}, R_{\text{N}}$)-1, as reported above for *rac*-2.

Catalytic procedure for the DA reaction between methacrolein and cyclopentadiene

At RT, in an NMR tube, to a solution of 1.16×10^{-3} or 2.32×10^{-3} mmol (5 or 10 mol%) of the corresponding catalyst in CD_2Cl_2 (0.5 mL), 2.0 μL (0.023 mmol) of methacrolein and 10 mg of 4 Å MS were added. After 5 min, 7.0 μL (0.081 mmol) of freshly distilled cyclopentadiene was added. After the indicated reaction times, the conversion and *exo/endo* ratio were determined by ^1H NMR. The enantiomeric ratio for the *exo* isomer was determined by integration of the ^1H NMR signals in presence of the chiral shift reagent (+)-Eu(hfc)₃. Major enantiomer (*R*), $\delta = 17.10$ ppm; minor enantiomer (*S*), $\delta = 19.09$ ppm.¹⁸

Catalytic procedure for the 1,3-dipolar cycloaddition reaction between methacrolein and *N*-benzylidenphenylamine-*N*-oxide

In an NMR tube, complex 2 (1.16×10^{-3} mmol (2.70 mg), 5 mol%) was dissolved in CD_2Cl_2 (0.2 mL) at −25 °C. Freshly distilled methacrolein (5 μL , 0.07 mmol) and 10.0 mg of activated 4 Å molecular sieves were added. After seeking the resulting suspension, a solution of *N*-benzylidenphenylamine-*N*-oxide (6.70 mg, 0.035 mmol) in CD_2Cl_2 (0.3 mL) was added. Regioselectivity was determined by the integration of the ^1H NMR signal of the C3 proton on the crude mixture in CD_2Cl_2 . Enantioselectivity was determined by the integration of the ^1H NMR signals of the diastereomeric (*S*)-methylbenzylimine derivatives.

Conflicts of interest

The authors declare no competing financial interests.

Acknowledgements

We thank the Ministerio de Ciencia, Innovación y Universidades (MCIU) of Spain, Agencia Estatal de Investigación (AEI) of Spain, Fondo Europeo de Desarrollo Regional (FEDER) (CTQ2018-095561-BI00 and PID2021-122406NB-I00) and Gobierno de Aragón (Grupo de Referencia: Catálisis Homogénea Enantioselectiva E05-20R) for financial support.

References

- (a) *Comprehensive Asymmetric Catalysis*, ed. E. N. Jacobsen, A. Pfaltz and H. Yamamoto, Springer, New York, 1999, vol. I–III; (b) *Catalytic Asymmetric Synthesis*, ed. I. Ojima, VCH, Weinheim, 2000; (c) R. Noyori, *Asymmetric Catalysis in Organic Synthesis*, John Wiley and Sons, New York, 1994; (d) P. J. Walsh and M. C. Kozlowski, *Fundamentals of Asymmetric Catalysis*, University Science Books, Sausalito, 2009.
- H. Brunner, *Acc. Chem. Res.*, 1979, **12**, 250–257.
- K. Muñiz and C. Bolm, *Chem.–Eur. J.*, 2000, **6**, 2309–2316.
- A. Werner, *Ber. Dtsch. Chem. Ges.*, 1911, **44**, 1887–1898.
- (a) L. Gong, M. Wenzel and E. Meggers, *Acc. Chem. Res.*, 2013, **46**, 2635–2644; (b) E. Meggers, *Eur. J. Inorg. Chem.*, 2011, 2911–2926; (c) E. Meggers, *Chem.–Eur. J.*, 2010, **16**, 752–758; (d) M. Fontecabe, O. Hamelin and S. Ménage, *Top. Organomet. Chem.*, 2005, **15**, 271–288.
- M. Chavarot, S. Ménage, O. Hamelin, F. Charnay, J. Pécaut and M. Fontecave, *Inorg. Chem.*, 2003, **42**, 4810–4816.
- (a) G. M. Fusi, S. Gazzola and U. Piarulli, *Adv. Synth. Catal.*, 2022, **364**, 696–714; (b) P. Dey, P. Rai and B. Maji, *ACS Org. Inorg. Au*, 2022, **2**, 99–125; (c) L. Zhang and E. Meggers, *Chem.–Asian J.*, 2017, **12**, 2335–2342; (d) L. Zhang and E. Meggers, *Acc. Chem. Res.*, 2017, **50**, 320–330; (e) Z.-Y. Cao, W. D. G. Brittain, J. S. Fossey and F. Zhou, *Catal. Sci. Technol.*, 2015, **5**, 3441–3451.
- (a) V. A. Larionov, B. L. Feringa and Y. N. Belokon, *Chem. Soc. Rev.*, 2021, **50**, 9715–9740; (b) A. Fanourakis, A. Philip,



- J. Docherty, P. Chuentragool and R. J. Phipps, *ACS Catal.*, 2020, **10**, 10672–10714; (c) S. K. Ghosh, A. Ehnobom, K. G. Lewis and J. A. Gladysz, *Coord. Chem. Rev.*, 2017, **350**, 30–48; (d) A. Ehnobom, S. K. Ghosh, K. G. Lewis and J. A. Gladysz, *Chem. Soc. Rev.*, 2016, **45**, 6799–6811; (e) L. Gong, L.-A. Chen and E. Meggers, *Angew. Chem., Int. Ed.*, 2014, **53**, 10868–10874.
- 9 (a) X. Huang and E. Meggers, *Acc. Chem. Res.*, 2019, **52**, 833–847; (b) H. Huo and E. Meggers, *Chimia*, 2016, **70**, 186–191; (c) E. Meggers, *Chem. Commun.*, 2015, **51**, 3290–3301.
- 10 (a) C. Ganzmann and J. A. Gladysz, *Chem.–Eur. J.*, 2008, **14**, 5397–5400; (b) W. J. Maximuck, C. Ganzmann, S. Alvi, K. R. Hooda and J. A. Gladysz, *Dalton Trans.*, 2020, **49**, 3680–3691.
- 11 (a) J. Hartung and R. H. Grubbs, *J. Am. Chem. Soc.*, 2013, **135**, 10183–10185; (b) J. Hartung, P. K. Dornan and R. H. Grubbs, *J. Am. Chem. Soc.*, 2014, **136**, 13029–13037.
- 12 K. Endo, Y. Liu, H. Ube, K. Nagata and M. Shionoya, *Nat. Commun.*, 2020, **11**, 6263.
- 13 (a) M. Carmona, R. Rodríguez, V. Passarelli and D. Carmona, *Organometallics*, 2019, **38**, 988–995; (b) J. Téllez, I. Méndez, F. Viguri, R. Rodríguez, F. J. Lahoz, P. García-Orduña and D. Carmona, *Organometallics*, 2018, **37**, 3450–3464; (c) M. Carmona, R. Rodríguez, V. Passarelli, F. J. Lahoz, P. García-Orduña and D. Carmona, *J. Am. Chem. Soc.*, 2018, **140**, 912–915; (d) M. Carmona, L. Tejedor, R. Rodríguez, V. Passarelli, F. J. Lahoz, P. García-Orduña and D. Carmona, *Chem.–Eur. J.*, 2017, **23**, 14532–14546; (e) M. Carmona, R. Rodríguez, I. Méndez, V. Passarelli, F. J. Lahoz, P. García-Orduña and D. Carmona, *Dalton Trans.*, 2017, **46**, 7332–7350.
- 14 (a) R. S. Cahn, C. Ingold and V. Prelog, *Angew. Chem., Int. Ed. Engl.*, 1966, **5**, 385–415; (b) V. Prelog and G. Helmchen, *Angew. Chem., Int. Ed. Engl.*, 1982, **21**, 567–583; (c) C. Lecomte, Y. Dusauso, J. Protas, J. Tirouflet and A. Dormond, *J. Organomet. Chem.*, 1974, **73**, 67–76. For the C/A convention for octahedral centres see ; (d) N. G. Connelly, T. Damhus, R. H. Hartshorn and A. T. Hutton, *Nomenclature of Inorganic Chemistry, IUPAC Recommendations*, RSC Publishing, Cambridge, UK, 2005, ch. IR-9.3.4.8, p. 189.
- 15 To simplify the notation of the stereochemical descriptors, we will label these diastereomers as $C_{Rh,RN}$ and $A_{Rh,SN}$. *R* and *S* refer to the configuration at the sp^3 nitrogen and *C* and *A* to the clockwise or anticlockwise arrangement of the donor atoms at the equatorial plane of the octahedral metal complex.
- 16 CCDC-2206804.†
- 17 Due to the nomenclature rules, in this transformation, retention of the configuration implies the change of the metal descriptor from *A* to *C*, and *vice versa*.
- 18 (a) K. Furuta, S. Shimizu, Y. Miwa and H. Yamamoto, *J. Org. Chem.*, 1989, **54**, 1481–1483; (b) J. W. Faller, X. Liu and J. Parr, *Chirality*, 2000, **12**, 325–337; (c) D. Carmona, M. P. Lamata, F. Viguri, R. Rodríguez, C. Barba, F. J. Lahoz, M. L. Martín, L. A. Oro and L. Salvatella, *Organometallics*, 2007, **26**, 6493–6496.
- 19 D. Carmona, M. P. Lamata, F. Viguri, R. Rodríguez, L. A. Oro, F. J. Lahoz, A. I. Balana, T. Tejero and P. Merino, *J. Am. Chem. Soc.*, 2005, **127**, 13386–13398.
- 20 (a) E. P. Kündig, C. M. Saudan and G. Bernardinelli, *Angew. Chem., Int. Ed.*, 1999, **38**, 1220–1223; (b) D. Carmona, C. Cativiela, S. Elipe, F. J. Lahoz, M. P. Lamata, M. P. López-Ram de Víu, L. A. Oro, C. Vega and F. Viguri, *Chem. Commun.*, 1997, 2351–2352; (c) A. J. Davenport, D. L. Davies, J. Fawcett, S. A. Garrat and D. R. J. Russell, *J. Chem. Soc., Dalton Trans.*, 2000, 4432–4441.

